

# RCS and Radar Propagation Near Offshore Wind Farms

Laith S Rashid\*, Anthony K Brown  
The University of Manchester, UK  
E-mail: l.rashid@manchester.ac.uk

## Introduction

Offshore wind farms cover large areas of open water and hence present potential hazards to navigation. Investigation into the interference by wind farms with ships' radar has confirmed that there may be an impact on radar producing spurious returns on displays caused by multiple reflections, as well as beam spreading and side-lobe detection due to the very high radar cross section of the wind turbine [2, 3].

The wind farm impact on marine radars has not been widely reported. Some past publications have touched on the subject [3, 7, 11] but there has been no accurate model in place to readily examine the effects of different farm geometries, tower shapes and turbine sizes. This paper discusses the radar propagation modeling near offshore wind farms including the methods used to model individual turbine mono and bi-static RCS, and the multiple reflections of radar signals within the wind farm. An initial qualitative comparison between the results of the model and measured data is provided.

## The Wind Turbine Model

Wind turbines are large structures that are typically made of GRP and/or carbon fiber composite components mounted on steel towers. Full physical optics modeling [1, 4, 8] of a typical turbine shows that the RCS can be in the order of 60 dBms ( $10^6 \text{ m}^2$ ) at 9.4 GHz which is of the same order as a large oil tanker broadside on.

Pinto [8] shows results of a full physical optics modeling of a wind turbine. This shows the variation in RCS with respect to the rotation angle of the blades and the yaw angle as defined in Figure 1. It was found that the tower constitutes by far the largest source of scatter (approx. 80%) followed by the blades (5% each). [7].

The problem of utilizing the physical optics model for a flexible wind farm calculation is largely one of scale. While RCS prediction of this size is possible clearly it is non trivial. An additional problem is in a wind farm adjacent turbines are in the near field of their neighbors and may be in the near field of the ship's radar antenna. This significantly increases computational effort.

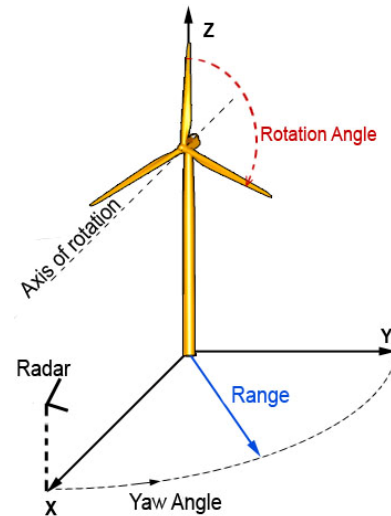


Figure 1: Modeling coordinate

Accordingly a simplified, approximate model has been developed to compute the monostatic and bistatic RCS of the tower as the dominant component and combined

with the PO model of the blade to provide a rapid calculation tool capable of positioning the blades at any rotation/yaw angle.

### Turbine RCS Model

The complete turbine is modeled as a set of sections as shown in Figure 2 below. The RCS values for sections including the nacelle, the blades and the nosecone across all yaw and rotation angles were taken from the full PO model, so that the shape of the blade is accurately taken into account. Each section is then assumed as a point scatterer positioned at the centre of the relevant section with phase referenced to this point. The tower is split into small cylindrical sections, so that the nearfield RCS can be calculated provided that the effective scattering centre for each section is known

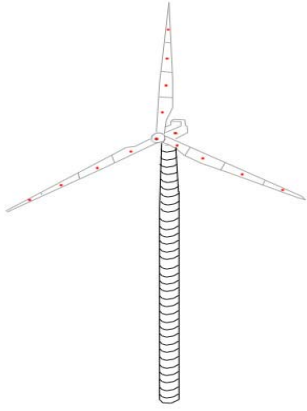


Figure 3: Segmented tower geometry.

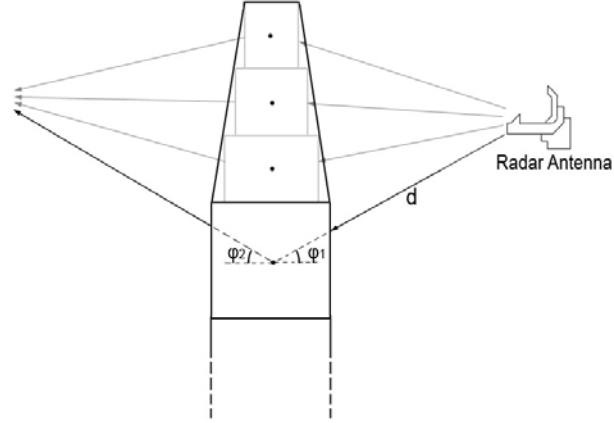


Figure 2: Segmented turbine model

We note both mono- and bi-static RCS prediction is required: The monostatic RCS of the tower is used to investigate issues such as the target spreading and side-lobe detection, while the bistatic RCS is required to predict the appearance of ghost targets due to multiple reflection issues.

The bistatic RCS of each tower section was obtained using standard simplified physical optics farfield RCS approximations of a cylinder [5, 9] given in Equation (1). Note that the monostatic RCS of the cylindrical section can be obtained by substituting  $\theta$  equals to zero, where  $\theta$  is the bistatic scattering angle.

$$\sigma_{bi} = krh^2 [\cos^2 \varphi_2 \cos(\theta/2) / \cos \varphi_1] \text{sinc}^2 [kh/2(\sin \varphi_1 + \sin \varphi_2)] \quad (1)$$

The phase reference point of each section is assumed to be at the surface of the cylindrical section since the section diameters are very large compared to the wavelength of the radar signal. With information about the radar height and the range, the distance to each segment  $d$  is calculated which is used to account for the phase contribution of individual segments.

Figure 3 shows a simplified segmented tower. Using the approximation discussed above, the complex field  $V_n$  value at any required for each segment is simply

$$V_n = [\sigma_n / (d_n / R)^2]^{1/2} \quad (2)$$

A complex summation over all segments leads to the required total bistatic RCS of the tower at a defined point to a given direction.

## Multiple Bounce Model

When ships are near a wind farm ghost targets appear on the radar display due to multiple reflections of radar signals within the farm. A ray tracing model has been implemented which calculates successful ray directions from the ship radar to each tower and the direction from any one tower to any other. The monostatic and bistatic RCS of the tower in the required directions is then obtained from the above model and the field reflected or diffracted to the next tower calculated.

The model uses a recursive technique whereby the reflected signal off the tower is traced through as many bounces needed until it reaches a defined threshold value below which it is considered insignificant. The model also allows for potential multiple bounces both from any tower to any other tower and from a nearby ship to the towers.

Sea clutter effects are included based on the GIT empirical models [6, 10], in addition, a single point sea surface multipath reflection is included.

## Results

In order to validate the turbine RCS model, the results were compared to the full physical optics model from [8]. Figure 5 shows the variation of the RCS around the turbine while maintaining the rotation angle at  $0^\circ$ .

The model shows a good correlation with the full PO model. At  $180^\circ$  the model peaks slightly higher than the PO model due to the shadowing effect from the tower and the nacelle, which is not included.

To illustrate the impact of wind farms on marine radar, the output of the model is in the form of a synthetic scan-converted display showing the radar returns in a color coded scale. The impact model has been compared to some available radar display images taken when visiting an offshore wind farm in North Wales.

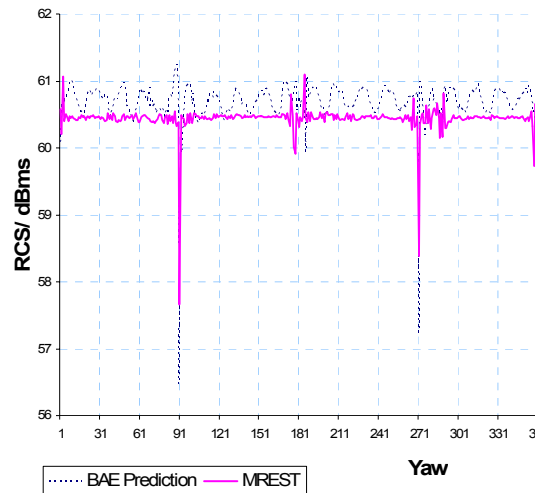


Figure 5: RCS variation around the turbine

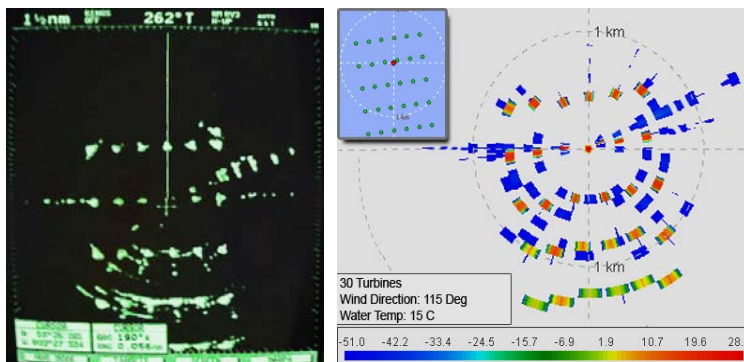


Figure 8: Measured data and model results

Figure 8 shows a picture of the actual radar display showing the effects of sidelobe detection, target spreading and multiple reflections of radar signals. When this scenario was modeled using the developed model, the locations of the wind turbines were set as closely as possible to that in the measurement.

The results show a good quantitative correlation between the model and the measurement is clear. There is a significant detection through the side lobes and the appearance of ghost targets is observed. The locations of these returns are very similar to that in the measured data. Differences in the detailed level of the side lobe detections may be caused by using an estimated azimuth antenna pattern rather than a measured pattern. The model also does not use any video processing algorithms or automatic gain and thresholding settings, which the shipborne radar was set to have.

### Conclusion

The radar model developed at the University of Manchester is designed to give a flexible, rapid and reasonably accurate calculation for application to a wide variety of wind farms. Initial comparison of results with measurements, demonstrates the ability to simulate the interference of wind farms with navigational radars. Further work is required to further validate predictions; however, it has a good qualitative correlation with pictures of a shipborne radar screen taken at the North Hoyle wind farm.

### Acknowledgements

This work has been partially funded by a DTI innovation award, which is a collaboration between BAE Systems Ltd, Vestas a/s, University of Sheffield and University of Manchester. The help of our partners is gratefully acknowledged.

### References

- [1] S Appleton, "Stealthy Wind Turbines, addressing the radar issue", *BWEA28*, 2006
- [2] R Baker. "BWEA Marine Radar Investigation", *BWEA28*, (2006).
- [3] C Brown, M. Howard, "Results of the electromagnetic investigations and assessments of marine radar, communications and position fixing systems undertaken at the North Hoyle wind farm by QinetiQ and the Maritime and Coastguard Agency", *MCA Report MNA 53/10/366*, Nov 2004.
- [4] H S Dabis, "Wind Turbine Electromagnetic Scatter Modelling using Physical Optics Techniques", *Renewable Energy*, **16** pp. 882-887, (1999).
- [5] E F Knott, J F Shaeffer and M T Tuley, *Radar Cross Section*, 2<sup>nd</sup> edition. Boston: Artech House, 1993
- [6] M L Meeks, *Radar Propagation at Low Altitudes*. Boston: Artech House, 1982
- [7] J Pinto, A. K. Brown, L. Rashid, "Requirements Capture Summary Report", *Stealth Technology for Wind Turbines*, TP/2/RT/6/I/10117 APPS2B, April 2006
- [8] J Pinto. "Stealth Technology for Wind Turbines - Addressing the Aviation and Marine Radar Issues", *BWEA28*, (2006).
- [9] G T Ruck, D E Barrick, *Radar Cross Section Handbook*, Vol 1. New York: Plenum Press, 1970
- [10] M I Skolnik, *Introduction to Radar Systems*, 2<sup>nd</sup> edition. New York: McGraw-Hill Book Company, 1980
- [11] D A Zolnick, "Calculating the Radar Cross Section from multiple Bounce Interaction", *Naval Research Labs*, USA (1993).